International Journal on Magnetic Particle Imaging
Vol 8, No 1, Suppl 1, Article ID 2203080, 3 Pages

Proceedings Article

Characterizing the Performance of Commercial Magnetic Particles for Magnetic Particle Imaging

Kim Hwang Yeo[a,*] · Irati Rodrigo[a,*] · Renesmee Kuo[a] · Prashant Chandrasekharan[a] · Benjamin Fellows[a] · Steven Conolly[a,b]

[a]Department of Bioengineering, University of California, Berkeley, California, USA
[b]Department of Electrical Engineering and Computer Sciences, University of California, Berkeley, California, USA
*These authors contributed equally
*Corresponding author, email: irati.rodrigo@berkeley.edu

Abstract

The properties of magnetic nanoparticles (MNPs) are key to the effectiveness of magnetic particle imaging (MPI). While commercial MNPs are used extensively in clinical and research applications, there are still challenges in understanding the effect of certain MNP properties on its resolution and sensitivity. Being able to understand these trends will enhance efforts in optimizing parameters in MNP production for specific applications. In this study, we looked at MNP core size, clustering, and coating and their effects on its FWHM, and compared the sensitivity of different commercial particles. We identified a trend in FWHM and MNP core size as well as effects of certain coating on FWHM.

I. Introduction

I.I. Background and Motivation

Magnetic particle imaging (MPI) is a tracer-based molecular imaging technique that directly detects and quantifies magnetic nanoparticle (MNP) tracers by exploiting their magnetization [1]. This imaging modality produces clinical-grade images with zero tissue signal attenuation, high contrast, high sensitivity, and high resolution. MPI is well-suited for clinical application such as angiography [2], lung perfusion [3], stem cell tracking [4],[5], white blood cell tracking [6], brain perfusion [7], gut bleed detection [8], cancer imaging [9], and localized magnetic hyperthermia [10].

The point spread function (PSF) and its corresponding full width at half maximum (FWHM) are key parameters for characterizing tracer performance in MPI because they describe the image spatial resolution of the MNPs [11]. The dosage requirements of tracers are dependent on the sensitivity of the respective tracers. In this abstract we aim to identify a trend in resolution in relation to particle core size and characterize the sensitivity of commercial particles using the arbitrary waveform relaxometer (AWR) [12].

II. Methods and materials

Six types of magnetic nanoparticles were used in this work: Synomag®-D, Perimag® (micromod Partikeltechnologie GmbH, Germany), NanoXact® Magnetite Nanoparticles – Polyvinylpyrrolidone (PVP) (nanoComposix, USA), SHP25, SMG30 (Ocean Nanotech, USA), and Vivotrax (Magnetic Insight, USA). NanoXact (NN), SMG30-01 (SMG), and SHP25-02 (SHP) are single-core

MNP type	Name	Diameter (nm)	Particle Type	Coating	FWHM (mT)	Relative Sensitivity
Synomag®-D	MS1	70	cluster	Dextran	2.8	1.66
	MS2	50	cluster	PEG 25	12.2	13.48
	MS3	50	cluster	Dextran	10.4	14.73
Perimag®	MP1	130	cluster	Dextran	4.4	1.08
NanoXact™	NN	16	cluster	PVP	10	3.74
SMG30	SMG	30	single core	PEG	18.6	0.56
SHP25	SHP	25	single core	COOH	16.1	7.31
Vivotrax	VT	4.2	cluster	Carboxydextran	7.6	1.00

Table 1: Key properties and results of particles evaluated in this work, *Particle diameters listed here are cluster diameter for cluster-type MNPs and core diameter for single-core MNPs respectively. The exception is Vivotrax, as it does not have well-defined cluster sizes.

particles while Synomag-D (MS1, MS2, MS3), Perimag (MP1), and Vivotrax (VT) are cluster-type particles. Their properties are listed in Table 1. The FWHM of each particle was evaluated from the PSF data obtained through the AWR.

For these measurements, a sinusoidal AC magnetic field at 20 kHz with field strengths up to 24 mT was applied. The actual concentrations of the samples were measured using the model 721 UV-VIS spectrophotometer. Prussian Blue assay was conducted to stain for iron using Sigma HT20-1KT Iron Stain Kit (Sigma Aldrich, USA), and Iron Standard for ICP (Sigma-Aldrich, USA) was used for calibration. 5, 10, and 25 uL of each sample was run through the AWR to obtain the peak signal voltage corresponding to the lowest FWHM for each MNP. Using the measured concentration values, a standard curve for each MNP was plotted to determine their sensitivity in V/g of iron. The relative sensitivity of each MNP was normalized to the sensitivity of VT (Figure 2).

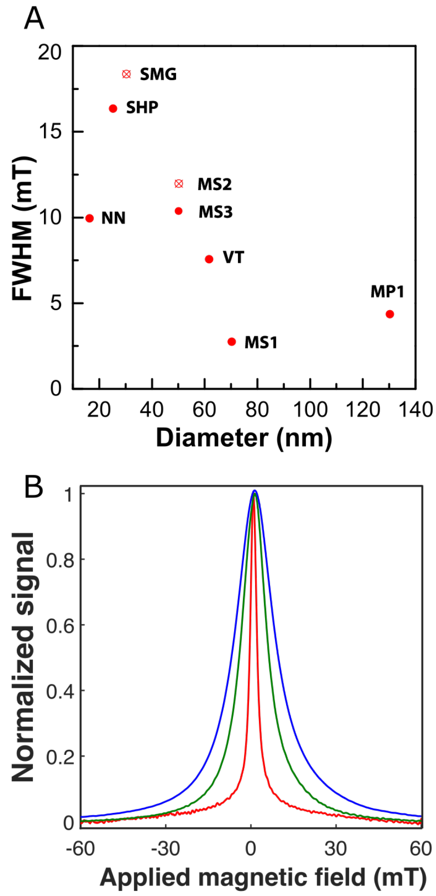

Figure 1: **(A)** Particle diameter is plotted against FWHM values. For this plot, the hydrodynamic diameter of VT is used. Particles marked with a [x] are coated with PEG25. **(B)** PSF curve of MS1 (red), MS3 (green), and SHP (blue).

III. Results and Discussion

As shown in Figure 1(a), the FWHM of single-core particles (SMG and SHP) increases with core diameter. On the other hand, the FWHM of cluster-type particles decreases significantly between 50 nm and 70 nm and increases again, reaching a value of 4.4 mT at sizes close to 130 nm. The differences in FWHM are also compared via the PSFs of MS1, MS3, and SHP in Figure 1(b). The FWHM values of all the tested particles are listed in Table 1.

The relative sensitivity of the MNP samples are shown in Figure 2. From the data obtained, there is no conclusive indication that the sensitivity of a MNP correlates with its size or surface chemistry. It should be noted that the sensitivity of the particles are analyzed based on the limited dataset obtained from the 2 to 24 mT drive field. It is observed that for some particles, there is a trade-off between image resolution and sensitivity.

Finally, effects of PEG25 surface coating on FWHM is observed. From this work, PEG25 coating appears to increase the FWHM of MNPs of similar size (see Figure 1(a)).

IV. Conclusion

The Langevin function predicts a cubic reduction in FWHM with an increase in magnetic core diameter. However, our previous work demonstrated a deviation from this Langevin theory due to relaxation wall effect [13], [14]. In the current abstract, larger-sized nanoparticles with clustered cores showed better FWHM in the sizes of 50-130 nm than the non-interacting single core nanoparticles of 25 nm in size. This potentially shows that interacting magnetic particles can improve MPI resolution and sensitivity.

From this work, we observe that multiple factors affect the FWHM of a MNP, such as core size and coating. It is worthwhile to note that while the FWHM of MNPs affect the resolution of MPI images, other factors such as

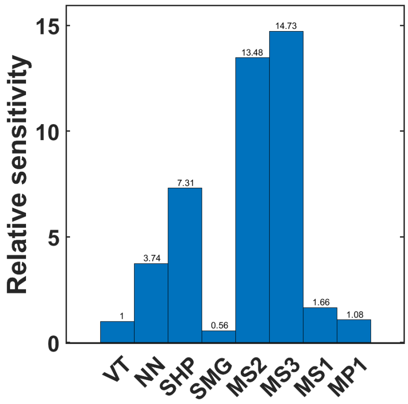

Figure 2: The relative sensitivity of each particle with respect to Vivotrax, in order of particle diameter.

coating, particle size, and sensitivity of the MNPs are important factors to be considered in specific applications. Further studies in this direction including clustering effects of MNPs can help identify a trend in characteristics that will aid in the selection and production of MNPs for targeted applications.

Acknowledgments

We gratefully acknowledge support from NIH grants R01s EB019458, EB024578, EB029822 and R44: EB029877, UC TRDRP grant 26IP-0049, M. Cook Chair, Bakar Fellowship, the Siebel fellowship, the UC Discovery Award, the Craven Fellowship from UC Berkeley Bioengineering, NSERC fellowship, as well as the NIH-T32 training, NSF fellowships and Gobierno Vasco from grant POS-2020-1-0028 (Programa de Perfeccionamiento de Personal Investigador Doctor).

Author's statement

Conflict of interest: Dr. Conolly is a co-founder of a startup company that manufactures and sells preclinical MPI scanners.

References

[1] B. Gleich and J. Weizenecker. Tomographic imaging using the nonlinear response of magnetic particles. *Nature*, 435(7046):1214–1217, 2005, doi:10.1038/nature03808.

[2] A. Mohtashamdolatshahi, H. Kratz, O. Kosch, R. Hauptmann, N. Stolzenburg, F. Wiekhorst, I. Sack, B. Hamm, M. Taupitz, and J. Schnorr. In vivo magnetic particle imaging: Angiography of inferior vena cava and aorta in rats using newly developed multicore particles. *Scientific Reports*, 10(1):17247, 2020, Bandiera_abtest: doi:10.1038/s41598-020-74151-4.

[3] X. Y. Zhou, K. E. Jeffris, E. Y. Yu, B. Zheng, P. W. Goodwill, P. Nahid, and S. M. Conolly. First In Vivo Magnetic Particle Imaging of Lung Perfusion in Rats. *Physics in medicine and biology*, 62(9):3510–3522, 2017, doi:10.1088/1361-6560/aa616c.

[4] B. Zheng, T. Vazin, P. W. Goodwill, A. Conway, A. Verma, E. Ulku Saritas, D. Schaffer, and S. M. Conolly. Magnetic Particle Imaging tracks the long-term fate of in vivo neural cell implants with high image contrast. *Scientific Reports*, 5(1):14055, 2015, doi:10.1038/srep14055.

[5] O. C. Sehl, J. J. Gevaert, K. P. Melo, N. N. Knier, and P. J. Foster. A Perspective on Cell Tracking with Magnetic Particle Imaging. *Tomography*, 6(4):315–324, 2020, doi:10.18383/j.tom.2020.00043.

[6] Surface protein targeted white blood cell tracking of inflammation using Magnetic Particle Imaging (WBC-MPI) - King Long Barry Fung - WMIC. (visited on 12/13/2021).

[7] M. Graeser, F. Thieben, P. Szwargulski, F. Werner, N. Gdaniec, M. Boberg, F. Griese, M. Möddel, P. Ludewig, D. van de Ven, O. M. Weber, O. Woywode, B. Gleich, and T. Knopp. Human-sized magnetic particle imaging for brain applications. *Nature Communications*, 10(1), 2019, doi:10.1038/s41467-019-09704-x.

[8] E. Y. Yu, P. Chandrasekharan, R. Berzon, Z. W. Tay, X. Y. Zhou, A. P. Khandhar, R. M. Ferguson, S. J. Kemp, B. Zheng, P. W. Goodwill, M. F. Wendland, K. M. Krishnan, S. Behr, J. Carter, and S. M. Conolly. Magnetic Particle Imaging for Highly Sensitive, Quantitative and Safe In Vivo Gut Bleed Detection in a Murine Model. *ACS nano*, 11(12):12067–12076, 2017, doi:10.1021/acsnano.7b04844.

[9] E. Y. Yu, M. Bishop, B. Zheng, R. M. Ferguson, A. P. Khandhar, S. J. Kemp, K. M. Krishnan, P. W. Goodwill, and S. M. Conolly. Magnetic Particle Imaging: A Novel in Vivo Imaging Platform for Cancer Detection. *Nano Letters*, 17(3):1648–1654, 2017, doi:10.1021/acs.nanolett.6b04865.

[10] Z. W. Tay, P. Chandrasekharan, A. Chiu-Lam, D. W. Hensley, R. Dhavalikar, X. Y. Zhou, E. Y. Yu, P. W. Goodwill, B. Zheng, C. Rinaldi, and S. M. Conolly. Magnetic Particle Imaging-Guided Heating in Vivo Using Gradient Fields for Arbitrary Localization of Magnetic Hyperthermia Therapy. *ACS Nano*, 12(4):3699–3713, 2018, Publisher: American Chemical Society. doi:10.1021/acsnano.8b00893.

[11] P. W. Goodwill and S. M. Conolly. The X-Space Formulation of the Magnetic Particle Imaging Process: 1-D Signal, Resolution, Bandwidth, SNR, SAR, and Magnetostimulation. *IEEE Transactions on Medical Imaging*, 29(11):1851–1859, 2010, Conference Name: IEEE Transactions on Medical Imaging. doi:10.1109/TMI.2010.2052284.

[12] Z. W. Tay, P. W. Goodwill, D. W. Hensley, L. A. Taylor, B. Zheng, and S. M. Conolly. A High-Throughput, Arbitrary-Waveform, MPI Spectrometer and Relaxometer for Comprehensive Magnetic Particle Optimization and Characterization. *Sci. Rep.*, 6:34180, 2016.

[13] Z. W. Tay, D. W. Hensley, E. C. Vreeland, B. Zheng, and S. M. Conolly. The Relaxation Wall: Experimental Limits to Improving MPI Spatial Resolution by Increasing Nanoparticle Core size. *Biomedical physics & engineering express*, 3(3):035003, 2017, doi:10.1088/2057-1976/aa6ab6.

[14] I. Rodrigo, J. Bryan, C. Saayuju, R. Kuo, K. Fung, C. Colson, Z. W. Tay, B. Fellows, Q. Huynh, P. Chandrasekharan, and S. M. Conolly, Comparing the performance of commercially available magnetic nanoparticles for magnetic particle imaging, presented at the World Molecular Imaging Congress, Virtual, 2021.

